Int J Clin Exp Med 2019;12(6):7305-7310
www.ijcem.com /ISSN:1940-5901/IJCEM0086524

Original Article

Evaluation of high-resolution susceptibility-weighted imaging in the diagnosis of cerebrovascular amyloidosis with cerebral microbleeds

Hui Su[1], Ke Wu[1], Xiaolin Zhu[1], Hao Shi[2]

[1]*Department of Medical Imaging, Tai'an Central Hospital of Shandong, Tai'an 271000, Shandong, China;* [2]*Department of Medical Imaging, Qianfoshan Hospital Affiliated to Shandong University, Jinan 250012, Shandong, China*

Received March 9, 2018; Accepted April 8, 2019; Epub June 15, 2019; Published June 30, 2019

Abstract: Objective: The goal of this study was to evaluate the diagnostic value of high-resolution susceptibility-weighted imaging (SWI) for cerebrovascular amyloidosis with cerebral microbleeds (CACM). Patients and methods: A total of 50 patients with CACM were enrolled and received the conventional magnetic resonance imaging (MRI) and high-resolution SWI (HR-SWI) examinations. The sensitivity, detection rate, and image quality of the two examination methods were compared. Results: A total of 105 lesions were diagnosed. The sensitivity of HR-SWI was 69.52% (73/105) and the detection rate was 96.00% (48/50), which were significantly higher than those of MRI [30.48% (32/105) and 68.00% (34/50), respectively] ($P < 0.05$). Furthermore, the total pass rate in the HR-SWI examination (90.00%) was significantly higher than that in MRI examination (64.00%) ($P < 0.05$). HR-SWI examination contributed to significantly higher ratio of high signals around the lesions [58.00% (29/50)] and lower mixed signals [6.00% (3/50)] than MRI group [4.00% (2/50) and [76.00% (38/50) respectively] ($P < 0.05$). HR-SWI sequences showed multiple low-signal areas with clear edges, or spot-like lesions. In MRI, T1-weighted images (T1WIs) were low signals and equisignals, which were relatively mixed, and some were manifested as ringlike, flake, and dotted T1 signals. T2WIs were mainly low and high signals, which were mixed. Conclusion: Compared with MRI, HR-SWI presented high detection rate and sensitivity in the diagnosis of CACM, and it is characterized with clear lesions as well as relatively high diagnostic value.

Keywords: Cerebrovascular amyloidosis, cerebral microbleeds, high-resolution susceptibility weighted imaging, magnetic resonance imaging, diagnosis

Introduction

As one of the cerebrovascular diseases, cerebrovascular amyloidosis frequently occurs in people aged over 60 years old, and its incidence rate is directly associated with the patient's age [1]. The disease in most patients is often diagnosed under the circumstance of cerebral hemorrhage. Its clinical manifestations lack specific performance, which are often accompanied by dementia and neuropsychiatric disorders. Additionally, the patients' life and health will be severely threatened in case of delayed treatment or intervention [2]. The basic characteristics of cerebrovascular amyloidosis with cerebral microbleeds (CACM) are multiple hemorrhages with no edema symptoms in peripheral brain tissues. The disease is difficult to be diagnosed and treated, and clinical application of the conventional magnetic resonance imaging (MRI) examination cannot fully identify the multiple strokes of the disease [3]. With improvement of imaging diagnostic techniques, high-resolution susceptibility-weighted imaging (HR-SWI) has been widely used to identify and diagnose central nervous disorders [4]. However, its role in the diagnosis of CACM remains poorly understood. In this study, 50 patients with CACM were recruited and comparative analyses of the features of the conventional MRI and HR-SWI examinations were performed, aiming to provide a scientific imaging basis for the clinical treatment of CACM.

Patients and methods

Patients

A total of 50 patients with CACM who were treated in our hospital from February 2016 to

October 2017 were selected, including 32 males and 18 females aged 51-87 years old, with an average age of (67.95 ± 7.42) years old. The following symptoms were observed at admission: headache (n = 50), meningeal irritation (n = 28), vomiting (n = 19) and dementia (n = 15). Among them, there were 21 cases with a history of hypertension. The study was approved by the Ethics Committee of our hospital and informed consents were obtained from all participants. The cohort of 50 patients received conventional MRI examination and High-resolution SWI (HR-SWI) examination.

Inclusion criteria

1) Patients aged ≥ 18 years old, 2) Patients definitely diagnosed with cerebrovascular amyloidosis with cerebral microbleeds by surgery, pathology and clinical examinations [5], 3) Patients who tolerated high-resolution SWI and MRI, and 4) Patients who were informed of the study content and methods, and voluntarily signed the informed consent.

Exclusion criteria

1) Patients with poor compliance to examinations, 2) Patients definitely diagnosed with intracranial space-occupying or other vascular diseases by surgery and pathology [6], 3) Patients with vascular malformations or hematological system diseases, 4) Patients who could not cooperative with examinations due to coma, 5) Patients with cerebral hemorrhage due to other causes in the past, or 6) Patients complicated with other severely impaired functions in multiple organs.

Conventional MRI examination

The superconducting MRI detection system [Signa 3.0T type, produced by General Electric (GE)] (Little Chalfont, England) was selected. Fluid attenuation inversion recovery sequence, spin echo T1-weighted images (T1WIs), and spin echo T2WIs were used for all patients. Sagittal and axial T1-fluid attenuation inversion recovery sequences: echo time (TE) was set to 23.4 ms, repetition time (TR) to 2632.6 ms, the interval to 1 mm, and the layer thickness to 6 mm. Axial T2WI: TE was set to 110.8 ms, TR to 4600.0 ms, interval to 1 mm, and the layer thickness to 6 mm. GE advantage 4.2 workstation was applied to process the intensity and phase images obtained during examinations.

High-resolution SWI (HR-SWI) examination

SWI parameters were set as follows: TE (25.8 ms), TR (41.5 ms), matrix (448 × 384), layer thickness (6 mm), field of view (FOV) (22 cm × 22 cm), and interval (1 mm). The image transmission workstation (GE advantage 4.2) (Little Chalfont, England) was used for processing, the phase images were obtained. Phase masks of phase images, low-pass filtering, and intensity projection were used for obtaining SWI.

Pathology analysis

Brain fiber surgery was used to remove the hematoma part. Cerebral hematoma tissues and the corresponding blood vessels were collected, and then sent to the Pathology Department in our hospital for histopathological analysis.

Observation indicators

The radiological images were analyzed by a deputy chief physician and a senior MRI physician. In cases of discrepancy, discussion was conducted until their opinions were consistent [7]. Evaluation content mainly included the lesion detection rate, sensitivity, image quality, and imaging features of HR-SWI and MRI examinations. According to the Likert scale, the image quality was classified into 5 grades, grade 5 (1 point for very poor image quality), grade 4 (2 points for general image quality), grade 3 (3 points for satisfying image quality), grade 2 (4 points for clear images), and grade 1 (5 points for very clear images). Grade 1-3 represented that the image quality was conformed to requirements [8, 9].

Statistical analysis

Statistical Product and Service Solutions (SPSS) 21.0 software was used to analyze data. Count data are expressed as case (n) and percentage (%), and detected via χ^2 test. Measurement data are expressed as mean ± standard deviation (SD). Student *t*-test was used for intergroup comparisons. $P < 0.05$ represented that the difference was statistically significant.

Results

Comparisons of the sensitivity and detection rate

A total of 105 lesions were detected. The lesion sensitivity of HR-SWI was 69.52% (73/105) and

Table 1. Comparison of the sensitivity and detection rates (n = 50)

Group	Sensitivity		Detection rate	
	The number of lesions	Sensitivity	Detected cases	Detection rate
MRI	32	30.48 (32/105)	34	68.00 (34/50)
High-resolution SWI	73	69.52 (73/105)	48	96.00 (48/50)
x^2	32.109		13.279	
p	< 0.001		< 0.001	

Table 2. Comparison of the Likert scale classification [n (%)]

Group	Very clear	Generally clear	Qualified	Poor	Extremely poor	Total pass rate
MRI (n = 50)	7 (14.00)	12 (24.00)	13 (26.00)	12 (24.00)	6 (12.00)	32 (64.00)
High-resolution SWI (n = 50)	12 (24.00)	18 (36.00)	15 (30.00)	4 (8.00)	1 (2.00)	45 (90.00)
x^2						9.543
p						< 0.001

Table 3. Signal features of the two examination methods [n (%)]

Group	High signal	Low signal	Mixed signal
MRI (n = 50)	2 (4.00)	10 (20.00)	38 (76.00)
High-resolution SWI (n = 50)	29 (58.00)	18 (36.00)	3 (6.00)
x^2	37.072	23.721	44.211

the detection rate was 96.00% (48/50), which were significantly higher than those of MRI [30.48% (32/105), 68.00% (34/50)] ($P < 0.05$) (**Table 1**).

Comparison of the Likert scale classification

The total Likert scale classification pass rate was compared between the two groups. The result revealed that the total pass rate of HR-SWI examination (90.00%) was significantly higher than that of MRI examination (64.00%) ($P < 0.05$) (**Table 2**).

Signal features of the two examination methods

HR-SWI examination showed significantly higher ratio of high signals around the lesions [58.00% (29/50)] and lower mixed signals [6.00% (3/50)], which was higher than that by MRI [4.00% (2/50) and 76.00% (38/50)], respectively ($P < 0.05$) (**Table 3**).

Analysis of HR-SWI features

HR-SWI sequence indicated that the edge of low-signal areas was clear, and bleeding lesions varied, including 24 cases with flake signals, 13 cases with irregularly shaped signals, 19 cases with oval or circular signals, and 6 cases with lobulated signals. Among them, two more forms of hematoma were found in 12 patients (**Figures 1**, **2**).

Analysis of MRI features

On MRI examination, T1WI performance data exhibited images that were mostly accompanied with low signals and mixed equisignals, and ringlike, flake, or dotted T1 signal diagrams. T2WI performance: Images were mostly low and high signals, which were mixed (**Figures 3**, **4**).

Discussion

Cerebrovascular amyloidosis with cerebral microbleeds is usually diagnosed due to intracranial hemorrhage. In most cases, no obvious symptoms and manifestations have been found in patients. Despite the differences in the size, site and the number of lesions, they are characterized by high recurrence rate and multiple strokes [10]. A previous study has reported that hematoma tissues oppressed the contralateral hemisphere of patients, which affected their awareness in combination with intracranial hypertension, and the decline degree was closely related to the site and size of intracerebral hematoma [11]. The main pathological basis of the disease is amyloid proteins

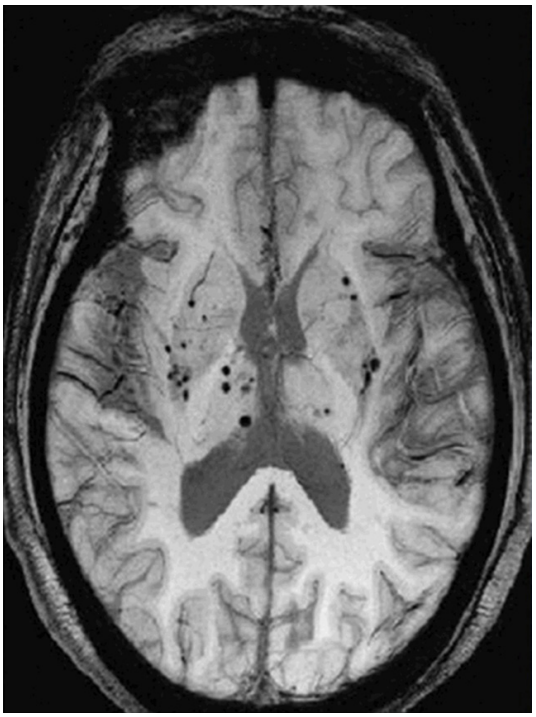

Figure 1. SWI of cerebrovascular amyloidosis with cerebral microbleeds.

Figure 2. SWI of the venous vascular structure.

which are deposited in the patient's cerebrovascular adventitia and middle layer. It thickens the intracranial vascular basement membrane. The patient's intracranial elastic layer rupture or stenosis will further result in micro-aneurysms and fibrinoid-like necrosis, thus leading to cerebrovascular amyloidosis with cerebral microbleeds [12]. At present, the clinical gold standard for the diagnosis of cerebrovascular amyloidosis with cerebral microbleeds is pathologic autopsy, but it is relatively difficult to perform clinically. Therefore, early and accurate diagnosis of the disease is of particular importance for treatment regimens in the later period.

High-resolution SWI is one of the new magnetic resonance contrast enhancement techniques, which can be used to obtain images by taking advantage of tissues with different magnetic susceptibilities, and its sensitivities to the deposition of iron and calcium, hemorrhage and veins with slower blood flow are comparatively high. In recent years, high-resolution SWI has been gradually applied in neurological examinations of cerebrovascular malformations, brain tumors, micro-cerebral hemorrhagic foci and brain tissue degeneration [13, 14]. In the present study, there were a total of 105 lesions detected by high-resolution SWI and conventional MRI, and the detection sensitivity of the former (69.52%) was significantly higher than that of the latter (30.48%), suggesting that compared with conventional MRI technique, high-resolution SWI presented a higher clinical sensitivity in cerebrovascular amyloidosis with cerebral microbleeds. Based on analysis, the reason might be that the pathology of the disease can be manifested as microbleed sites with the diameter < 5 mm which is formed by local plasma extravasation, and there are a certain amount of paramagnetic substances in the lesion, such as heme and deoxyhemoglobin, thus causing the inhomogeneity of local magnetic fields in intracranial lesions [15]. The main shortcoming of MRI is that its sensitivity to inhomogeneity is low without obvious signal characteristic, and the multiple strokes of cerebrovascular amyloidosis with cerebral microbleeds are difficult to be identified by it. Therefore, certain rates of misdiagnosis and missed diagnosis exist in clinical diagnosis of this disease [16]. However, high-resolution SWI can effectively reduce the negative impact of magnetic field inhomogeneity on the phase through high resolution, three-dimensional acquisition and the wave-layer reconstruction of gradient echo sequences, as well as post-pro-

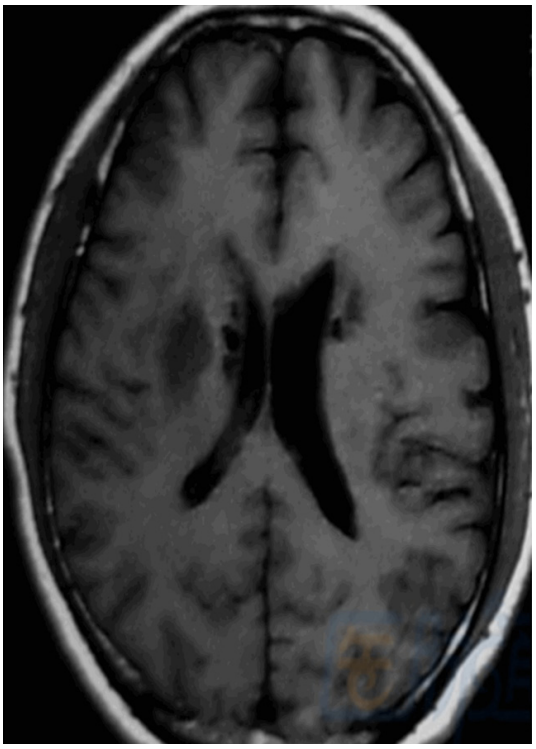

Figure 3. T1WI performance in MRI.

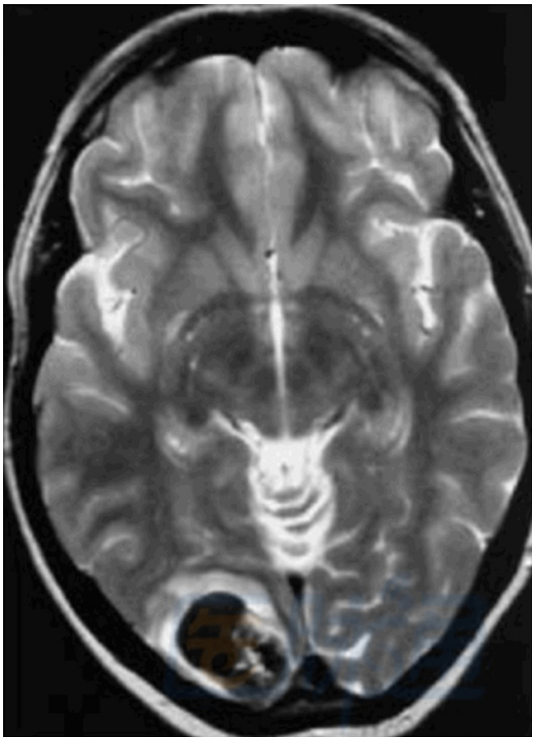

Figure 4. T2WI performance in MRI.

cessing of system images. It further facilitates to reduce or avoid the low sensitivity of conventional MRI technique to some extent [17]. In addition, the application of minimal signal intensity projection and assistive techniques for the three-dimensional reconstruction such as phase-weighted technique can effectively compensate for the deficiency of conventional MRI technique in detecting microbleed lesions.

In addition, this study also revealed that the Likert scale pass rate of high-resolution SWI reached as high as 90.00%, which was significantly higher than that of MRI (64.00%). As for imaging features, high-resolution SWI sequences showed multiple low-signal areas with clear edges, or spot-like lesions. In MRI, T1WIs were mostly profiled with low signals and equisignals, which were relatively mixed, and some were manifested as ringlike, flake, and dotted T1 signals. T2WIs were mainly mixed signals with poor image quality. As such, compared with conventional MRI, high-resolution SWI is conducive to improve the image quality, and clearly shows the site and severity of the lesion. It thus provides accurate imaging data for reference in the clinical diagnosis, which is analyzed to be related to the high-resolution three-dimensional gradient echo imaging technique of high-resolution SWI. This technique can achieve poor flow in three directions, effectively differentiating microbleed low-signal venous cross sections from cerebral ones, and uses the obtained phase images to distinguish cerebral calcified lesions in patients. Therefore the diagnostic accuracy and sensitivity of this technique have been improved [18].

Conclusion

In summary, compared with the conventional MRI examination, high-resolution SWI presents a high lesion detection rate and sensitivity in the diagnosis of cerebrovascular amyloidosis with cerebral microbleeds, which provides potential in the clinical diagnosis.

Disclosure of conflict of interest

None.

Address correspondence to: Dr. Hao Shi, Department of Medical Imaging, Qianfoshan Hospital Affiliated to Shandong University, 16766, Jingshi Road, Jinan 250012, Shandong, China. Tel: +86-531-82968900; Fax: +86-531-82968900; E-mail: haoshi2td@163.com

References

[1] Raposo N and Sonnen JA. Amyloid-PET in cerebral amyloid angiopathy: detecting vascular amyloid deposits, not just blood. Neurology 2017; 89: 1437-1438.

[2] Raz N, Daugherty AM, Sethi SK, Arshad M and Haacke EM. Erratum to: age differences in arterial and venous extra-cerebral blood flow in healthy adults: contributions of vascular risk factors and genetic variants. Brain Struct Funct 2017; 222: 2919-2920.

[3] Wintermark M, Hills NK, DeVeber GA, Barkovich AJ, Bernard TJ, Friedman NR, Mackay MT, Kirton A, Zhu G, Leiva-Salinas C, Hou Q, Fullerton HJ; VIPS Investigators. Clinical and imaging characteristics of arteriopathy subtypes in children with arterial ischemic stroke: results of the VIPS study. AJNR Am J Neuroradiol 2017; 38: 2172-2179.

[4] Szarka N, Amrein K, Horvath P, Ivic I, Czeiter E, Buki A, Koller A and Toth P. Hypertension-induced enhanced myogenic constriction of cerebral arteries is preserved after traumatic brain injury. J Neurotrauma 2017; 34: 2315-2319.

[5] Song P, Qin J, Lun H, Qiao P, Xie A and Li G. Magnetic resonance imaging (MRI) and digital subtraction angiography investigation of childhood moyamoya disease. J Child Neurol 2017; 32: 1027-1034.

[6] Ohtomo R, Bannai T, Ohtomo G, Shindo A, Tomimoto H, Tsuji S and Iwata A. Cilostazol alleviates white matter degeneration caused by chronic cerebral hypoperfusion in mice: implication of its mechanism from gene expression analysis. Neurosci Lett 2018; 662: 247-252.

[7] Lv P, Zhao M, Liu Y, Jin H, Cui W, Fan C, Teng Y, Zheng L and Huang Y. Apolipoprotein C-III in the high-density lipoprotein proteome of cerebral lacunar infarction patients impairs its anti-inflammatory function. Int J Mol Med 2018; 41: 61-68.

[8] Kim SK, Baek BH, Lee YY and Yoon W. Clinical implications of CT hyperdense artery sign in patients with acute middle cerebral artery occlusion in the era of modern mechanical thrombectomy. J Neurol 2017; 264: 2450-2456.

[9] Kalman M, Toth L, Szollosi D, Oszwald E, Mahalek J and Sadeghian S. Correlation between extravasation and alterations of cerebrovascular laminin and beta-dystroglycan immunoreactivity following cryogenic lesions in rats. J Neuropathol Exp Neurol 2017; 76: 929-941.

[10] Kralik SF, Watson GA, Shih CS, Ho CY, Finke W and Buchsbaum J. Radiation-induced large vessel cerebral vasculopathy in pediatric patients with brain tumors treated with proton radiation therapy. Int J Radiat Oncol Biol Phys 2017; 99: 817-824.

[11] Wan CC, Chen DY, Tseng YC, Yan FX, Lee KY, Chiang CH and Chen CJ. Fluid-attenuated inversion recovery vascular hyperintensities in predicting cerebral hyperperfusion after intracranial arterial stenting. Neuroradiology 2017; 59: 791-796.

[12] Mejia P, Trevino-Villarreal JH, Reynolds JS, De Niz M, Thompson A, Marti M and Mitchell JR. A single rapamycin dose protects against late-stage experimental cerebral malaria via modulation of host immunity, endothelial activation and parasite sequestration. Malar J 2017; 16: 455.

[13] Puy L, De Guio F, Godin O, Duering M, Dichgans M, Chabriat H and Jouvent E. Cerebral microbleeds and the risk of incident ischemic stroke in CADASIL (cerebral autosomal dominant arteriopathy with subcortical infarcts and leukoencephalopathy). Stroke 2017; 48: 2699-2703.

[14] Matsumi A, Takenaka R, Ando C, Sato Y, Takei K, Yasutomi E, Okanoue S, Oka S, Kawai D, Kataoka J, Takemoto K, Tsugeno H, Fujiki S and Kawahara Y. Preoperative pulmonary function tests predict aspiration pneumonia after gastric endoscopic submucosal dissection. Dig Dis Sci 2017; 62: 3084-3090.

[15] Lee TM, Vargas A, Dua S and Dafer RM. Cerebral infarctions following palliative transarterial chemoembolization with embozene of a vertebral body metastatic tumor. J Stroke Cerebrovasc Dis 2017; 26: e224-e225.

[16] Park HK, Kim BJ, Han MK, Park JM, Kang K, Lee SJ, Kim JG, Cha JK, Kim DH, Nah HW, Park TH, Park SS, Lee KB, Lee J, Hong KS, Cho YJ, Lee BC, Yu KH, Oh MS, Kim JT, Choi KH, Kim DE, Ryu WS, Choi JC, Johansson S, Lee SJ, Lee WH, Lee JS, Lee J, Bae HJ; CRCS-K Investigators. One-year outcomes after minor stroke or high-risk transient ischemic attack: korean multicenter stroke registry analysis. Stroke 2017; 48: 2991-2998.

[17] Carluccio MA, Di Donato I, Pescini F, Battaglini M, Bianchi S, Valenti R, Nannucci S, Franci B, Stromillo ML, De Stefano N, Inzitari D, Pantoni L, Nuti R, Federico A, Gonnelli S and Dotti MT. Vitamin D levels in cerebral autosomal dominant arteriopathy with subcortical infarcts and leukoencephalopathy (CADASIL). Neurol Sci 2017; 38: 1333-1336.

[18] Hardigan T, Hernandez C, Ward R, Hoda MN and Ergul A. TLR2 knockout protects against diabetes-mediated changes in cerebral perfusion and cognitive deficits. Am J Physiol Regul Integr Comp Physiol 2017; 312: R927-R937.